^{112}Sn(^{58}Ni,3pγ) 2003Jo06

History

Type	Author	Citation	Literature Cutoff Date
Full Evaluation	Balraj Singh and Jun Chen	NDS 191,1 (2023)	22-Aug-2023

2003Jo06: E=265 MeV ^{58}Ni beam was produced from the University of Jyvaskyla Accelerator. Target was 500 μg/cm^2 93.2% enriched self-supporting ^{112}Sn. Measured Eγ, Iγ, $\gamma\gamma$-coin, (recoils)γ-coin, γ anisotropy using the Jurosphere array comprising 13 Eurogam-type and 12 TESSA-type escape-suppressed Ge detectors. Two additional TESSA-type Ge detectors were positioned inside the Eurogam suppression shields. Fission products and primary scattered beam particles were separated from fusion evaporation residues by the RITU gas-filled recoil separator at the cyclotron facility of University of Jyvaskyla. Recoil-decay tagging method. Deduced high-spin levels, J^π, band structures, alignments, configurations, and B(M1)/B(E2) ratios.
Additional information 1.

^{167}Re Levels

Quasiparticle Labels:
A=$\nu i_{13/2}$1/2[660]; α=+1/2.
B=$\nu i_{13/2}$1/2[660]; α=−1/2.
E=$\nu h_{9/2}$5/2[523]; α=+1/2.
B_p=$\pi h_{11/2}$9/2[514]; α=+1/2.
A_p=$\pi h_{11/2}$9/2[514]; α=−1/2.

E(level)[†]	J^π[‡]	E(level)[†]	J^π[‡]	E(level)[†]	J^π[‡]	E(level)[†]	J^π[‡]
0.0+x[#]	(9/2$^-$)	1576.0+x[c] *9*	(19/2$^-$)	2390.0+x?[c] *16*	(27/2$^-$)	3146.3+x[a] *19*	(35/2$^+$)
91.6+x[@] *1*	(11/2$^-$)	1662.8+x[#] *10*	(21/2$^-$)	2431.3+x[#] *11*	(25/2$^-$)	3267.3+x[#] *16*	(33/2$^-$)
364.2+x[#] *6*	(13/2$^-$)	1695.0+x[d] *10*	(21/2$^-$)	2478.8+x[&] *18*	(29/2$^+$)	3436.3+x[&] *19*	(37/2$^+$)
600.9+x[@] *7*	(15/2$^-$)	1758.0+x[b] *10*	(21/2$^-$)	2660.1+x[a] *18*	(31/2$^+$)	3487.3+x[@] *16*	(35/2$^-$)
958.2+x[#] *8*	(17/2$^-$)	1959.0+x[c] *11*	(23/2$^-$)	2742.2+x[@] *12*	(27/2$^-$)	3744.3+x[#] *17*	(37/2$^-$)
1240.4+x[@] *9*	(19/2$^-$)	1971.2+x[@] *11*	(23/2$^-$)	2861.2+x *13*	(27/2$^-$)	3777.3+x[a] *20*	(39/2$^+$)
1304.0+x[d] *9*	(19/2$^-$)	2008.0+x[d] *11*	(23/2$^-$)	2882.4+x[&] *18*	(33/2$^+$)	4035.3+x[@] *17*	(39/2$^-$)
1364.6+x[c] *9*	(15/2$^-$)	2166.0+x[b] *12*	(25/2$^-$)	2947.3+x[#] *12*	(29/2$^-$)	4120.3+x[&] *21*	(41/2$^+$)
1452.8+x[b] *8*	(17/2$^-$)	2325.0+x[a] *16*	(27/2$^+$)	3082.3+x[@] *14*	(31/2$^-$)	4366.3+x[#] *20*	(41/2$^-$)

[†] From a least-squares fit to γ-ray energies.
[‡] As assigned by 2003Jo06, based on band associations, decay modes, and angular asymmetry ratios for selected transitions.
[#] Band(A): $A_p \rightarrow A_pAB$. A_p at low spins; A_pAB at high spins.
[@] Band(a): $B_p \rightarrow B_pAB$. B_p at low spins; B_pAB at high spins.
[&] Band(B): A_pAE.
[a] Band(b): B_pAE.
[b] Band(C): Band based on (17/2$^-$). π9/2[514]$\otimes\gamma-$vibration or π5/2[402] coupled to 2-quasineutron configuration of negative parity; α=+1/2.
[c] Band(c): Band based on (15/2$^-$). π9/2[514]$\otimes\gamma-$vibration or π5/2[402] coupled to 2-quasineutron configuration of negative parity; α=−1/2.
[d] Seq.(D): γ cascade based on (19/2$^-$).

^{112}Sn(^{58}Ni,3pγ) 2003Jo06 (continued)

γ(^{167}Re)

Angular asymmetry intensity ratios were measured as R(θ)=Iγ(157.6°)/Iγ(79°+101°), the values are plotted in Fig. 4 of the paper. Multipolarities were assigned from comparison with known stretched quadrupole (E2) and stretched dipole (E1) transitions in ^{168}Os, with R(θ)=0.84 *3* for stretched quadrupole and 0.56 *3* for stretched dipole. Values listed in this dataset have been digitized by evaluators from Fig. 4 in 2003Jo06.

E_γ [†]	E_i(level)	J_i^π	E_f	J_f^π	Mult. [‡]	Comments
86 *1*	2947.3+x	(29/2⁻)	2861.2+x	(27/2⁻)		
88 *1*	1452.8+x	(17/2⁻)	1364.6+x	(15/2⁻)		
91.6 *1*	91.6+x	(11/2⁻)	0.0+x	(9/2⁻)	D	R(θ)=0.46 *2*.
123 *1*	1576.0+x	(19/2⁻)	1452.8+x	(17/2⁻)		
135 *1*	3082.3+x	(31/2⁻)	2947.3+x	(29/2⁻)	D	R(θ)=0.34 *2*.
154 *1*	2478.8+x	(29/2⁺)	2325.0+x	(27/2⁺)	D	R(θ)=0.52 *2*.
159 *1*	2325.0+x	(27/2⁺)	2166.0+x	(25/2⁻)		
181 *1*	2660.1+x	(31/2⁺)	2478.8+x	(29/2⁺)		
182 *1*	1758.0+x	(21/2⁻)	1576.0+x	(19/2⁻)	D	R(θ)=0.48 *2*, could be for 182 and 181 γ rays, but the 182γ from (21/2⁻) level is more intense than 181γ from (31/2⁺) level.
185 *1*	3267.3+x	(33/2⁻)	3082.3+x	(31/2⁻)		
201 *1*	1959.0+x	(23/2⁻)	1758.0+x	(21/2⁻)	D	R(θ)=0.49 *2*.
205 *1*	2947.3+x	(29/2⁻)	2742.2+x	(27/2⁻)		
207 *1*	2166.0+x	(25/2⁻)	1959.0+x	(23/2⁻)	D	R(θ)=0.51 *2*, could be for 207 and 205 γ rays, but 207γ from (25/2⁻) level is more intense than 205γ from (29/2⁻) level.
220 *1*	3487.3+x	(35/2⁻)	3267.3+x	(33/2⁻)		
222 *1*	2882.4+x	(33/2⁺)	2660.1+x	(31/2⁺)		
224 [@] *1*	2390.0+x?	(27/2⁻)	2166.0+x	(25/2⁻)		
237 *1*	600.9+x	(15/2⁻)	364.2+x	(13/2⁻)		
242 *1*	1695.0+x	(21/2⁻)	1452.8+x	(17/2⁻)		
257 *1*	3744.3+x	(37/2⁻)	3487.3+x	(35/2⁻)		
264 *1*	3146.3+x	(35/2⁺)	2882.4+x	(33/2⁺)		
272 [#] *1*	364.2+x	(13/2⁻)	91.6+x	(11/2⁻)	D	R(θ)=0.59 *1*, could be for both the 272 γ rays, but the γ from (13/2⁻) level is more intense than the one from (19/2⁻) level.
272 [#] *1*	1576.0+x	(19/2⁻)	1304.0+x	(19/2⁻)		
282 *1*	1240.4+x	(19/2⁻)	958.2+x	(17/2⁻)		
290 *1*	3436.3+x	(37/2⁺)	3146.3+x	(35/2⁺)		
291 *1*	4035.3+x	(39/2⁻)	3744.3+x	(37/2⁻)		
305 *1*	1758.0+x	(21/2⁻)	1452.8+x	(17/2⁻)		
308 *1*	1971.2+x	(23/2⁻)	1662.8+x	(21/2⁻)		
311 *1*	2742.2+x	(27/2⁻)	2431.3+x	(25/2⁻)		
313 *1*	2008.0+x	(23/2⁻)	1695.0+x	(21/2⁻)		
331 *1*	4366.3+x	(41/2⁻)	4035.3+x	(39/2⁻)		
335 *1*	2660.1+x	(31/2⁺)	2325.0+x	(27/2⁺)		
336 *1*	1576.0+x	(19/2⁻)	1240.4+x	(19/2⁻)		
340 *1*	3082.3+x	(31/2⁻)	2742.2+x	(27/2⁻)		
341 *1*	3777.3+x	(39/2⁺)	3436.3+x	(37/2⁺)		
343 *1*	4120.3+x	(41/2⁺)	3777.3+x	(39/2⁺)		
346 [@] *1*	1304.0+x	(19/2⁻)	958.2+x	(17/2⁻)		
357 *1*	958.2+x	(17/2⁻)	600.9+x	(15/2⁻)		
365 *1*	364.2+x	(13/2⁻)	0.0+x	(9/2⁻)		
383 *1*	1959.0+x	(23/2⁻)	1576.0+x	(19/2⁻)		
391 *1*	1695.0+x	(21/2⁻)	1304.0+x	(19/2⁻)		
404 *1*	2882.4+x	(33/2⁺)	2478.8+x	(29/2⁺)		
405 *1*	3487.3+x	(35/2⁻)	3082.3+x	(31/2⁻)		
408 *1*	2166.0+x	(25/2⁻)	1758.0+x	(21/2⁻)		

Continued on next page (footnotes at end of table)

^{112}Sn(^{58}Ni,3pγ) 2003Jo06 (continued)

γ(^{167}Re) (continued)

E_γ †	E_i(level)	J^π_i	E_f	J^π_f	Mult.‡	Comments
422 *1*	1662.8+x	(21/2⁻)	1240.4+x	(19/2⁻)		
454 *1*	1758.0+x	(21/2⁻)	1304.0+x	(19/2⁻)		
460 *1*	2431.3+x	(25/2⁻)	1971.2+x	(23/2⁻)		
477 *1*	3744.3+x	(37/2⁻)	3267.3+x	(33/2⁻)		
486 *1*	3146.3+x	(35/2⁺)	2660.1+x	(31/2⁺)		
494 *1*	1452.8+x	(17/2⁻)	958.2+x	(17/2⁻)		
509 *1*	600.9+x	(15/2⁻)	91.6+x	(11/2⁻)		
516 *1*	2947.3+x	(29/2⁻)	2431.3+x	(25/2⁻)		
548 *1*	4035.3+x	(39/2⁻)	3487.3+x	(35/2⁻)		
554 *1*	3436.3+x	(37/2⁺)	2882.4+x	(33/2⁺)		
594 *1*	958.2+x	(17/2⁻)	364.2+x	(13/2⁻)	Q	R(θ)=0.81 *4*.
618 *1*	1576.0+x	(19/2⁻)	958.2+x	(17/2⁻)		
631 *1*	3777.3+x	(39/2⁺)	3146.3+x	(35/2⁺)		
640 *1*	1240.4+x	(19/2⁻)	600.9+x	(15/2⁻)		
684 *1*	4120.3+x	(41/2⁺)	3436.3+x	(37/2⁺)		
703 *1*	1304.0+x	(19/2⁻)	600.9+x	(15/2⁻)	Q	R(θ)=0.85 *3*, could be for 703, 704 and 705 γ rays, but the 703γ from (19/2⁻) level is more intense than 705γ from (21/2⁻) level, and 704γ is very weak.
704 *1*	2008.0+x	(23/2⁻)	1304.0+x	(19/2⁻)		
705 *1*	1662.8+x	(21/2⁻)	958.2+x	(17/2⁻)		
731 *1*	1971.2+x	(23/2⁻)	1240.4+x	(19/2⁻)	Q	R(θ)=1.03 *5*.
736 *1*	2431.3+x	(25/2⁻)	1695.0+x	(21/2⁻)		
764 *1*	1364.6+x	(15/2⁻)	600.9+x	(15/2⁻)		
768@ *1*	2008.0+x	(23/2⁻)	1240.4+x	(19/2⁻)		
769 *1*	2431.3+x	(25/2⁻)	1662.8+x	(21/2⁻)		
771 *1*	2742.2+x	(27/2⁻)	1971.2+x	(23/2⁻)		
852 *1*	1452.8+x	(17/2⁻)	600.9+x	(15/2⁻)		
890 *1*	2861.2+x	(27/2⁻)	1971.2+x	(23/2⁻)	Q	R(θ)=0.91 *7*.
975 *1*	1576.0+x	(19/2⁻)	600.9+x	(15/2⁻)		
1000 *1*	1364.6+x	(15/2⁻)	364.2+x	(13/2⁻)		
1089 *1*	1452.8+x	(17/2⁻)	364.2+x	(13/2⁻)		

† $\Delta E\gamma$ assigned as 1.0 keV based on a general statement by 2003Jo06, except for 91.6γ.
‡ Assigned by the evaluators from angular asymmetry ratios from 2003Jo06 as given under comments; not given in 2003Jo06.
# Multiply placed.
@ Placement of transition in the level scheme is uncertain.

$^{112}Sn(^{58}Ni,3p\gamma)$ 2003Jo06

Level Scheme

Legend

γ Decay (Uncertain)

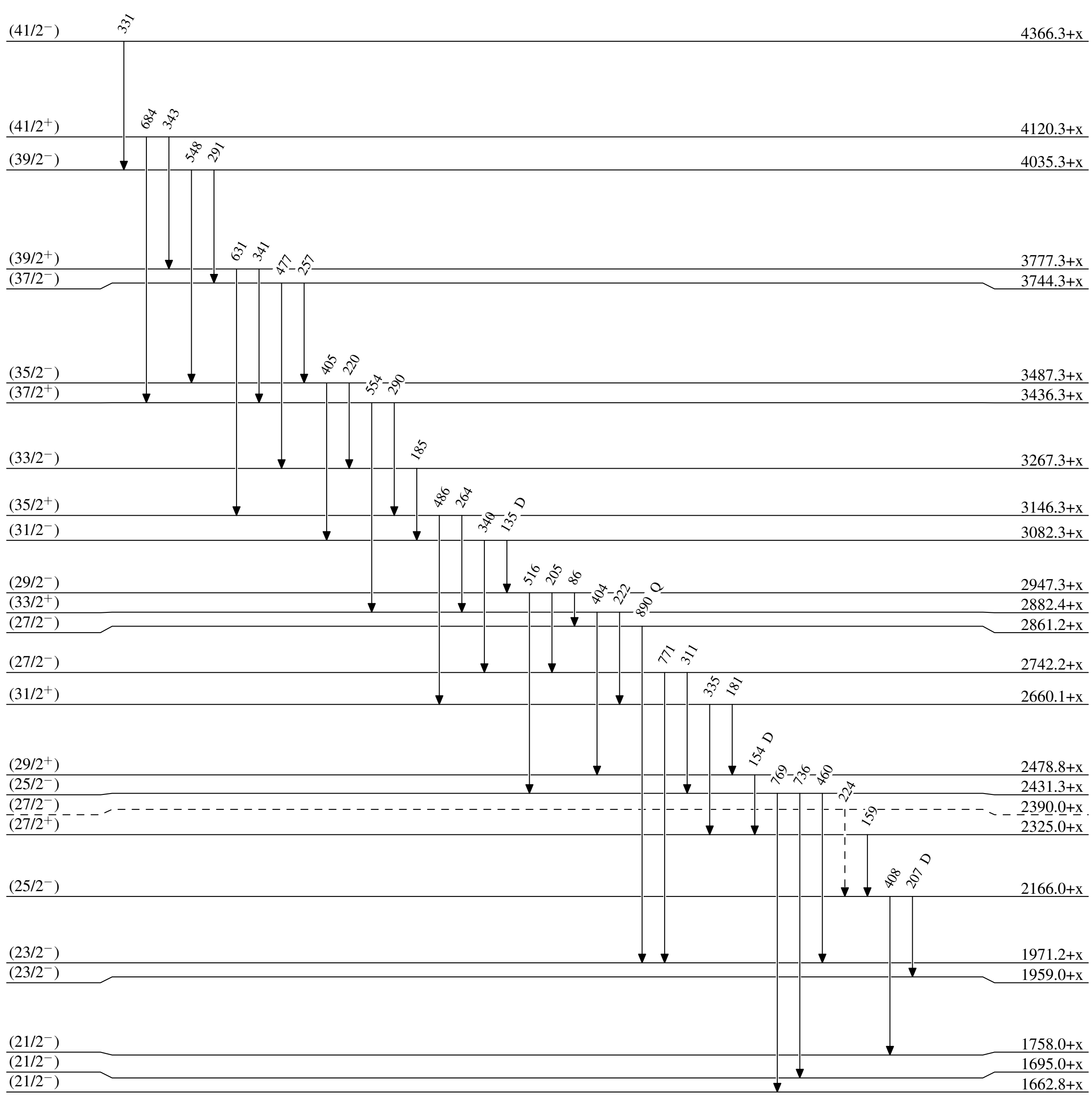

$^{167}_{75}Re_{92}$

$^{112}Sn(^{58}Ni,3p\gamma)$ 2003Jo06

Level Scheme (continued)

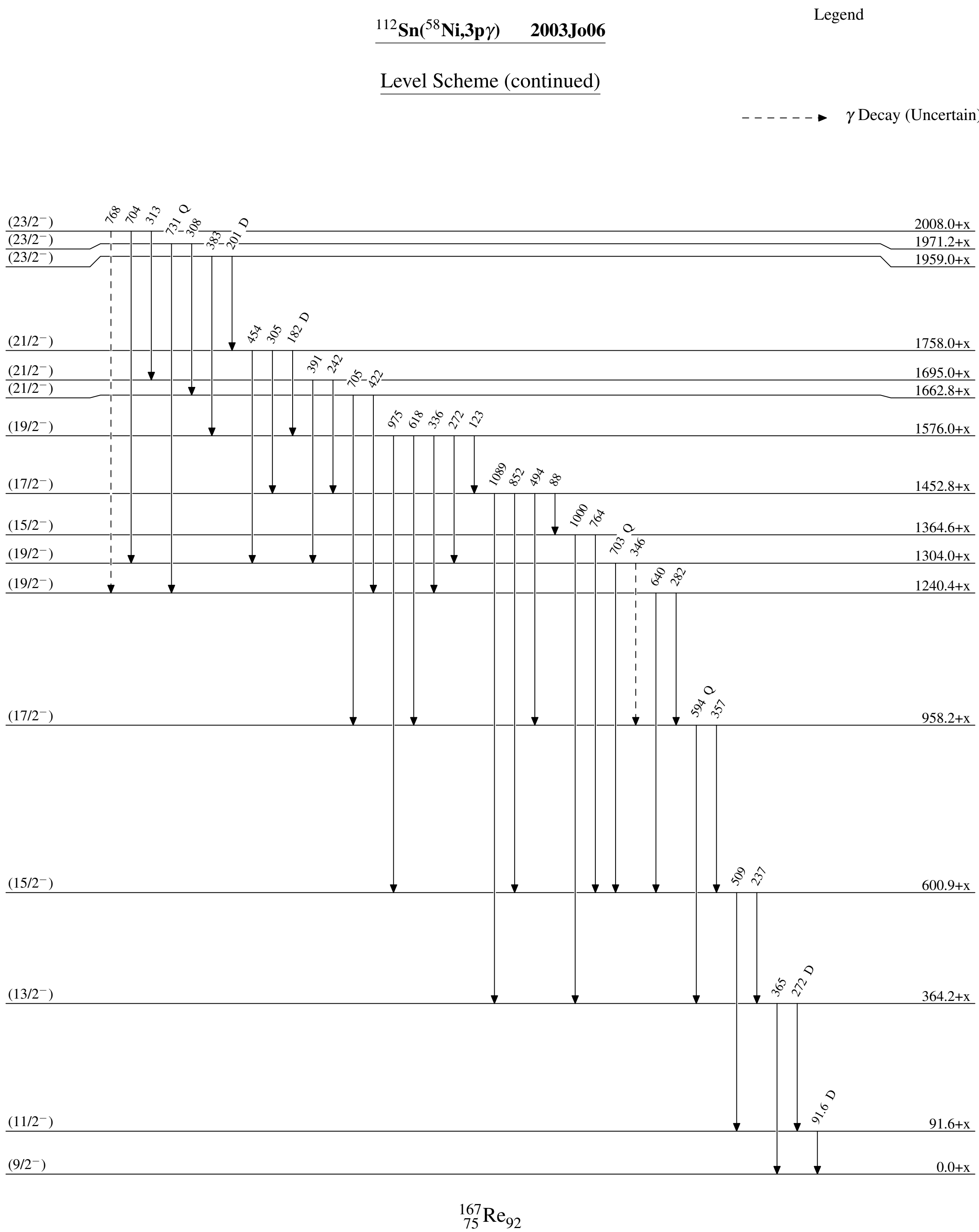

$^{112}Sn(^{58}Ni,3p\gamma)$ 2003Jo06

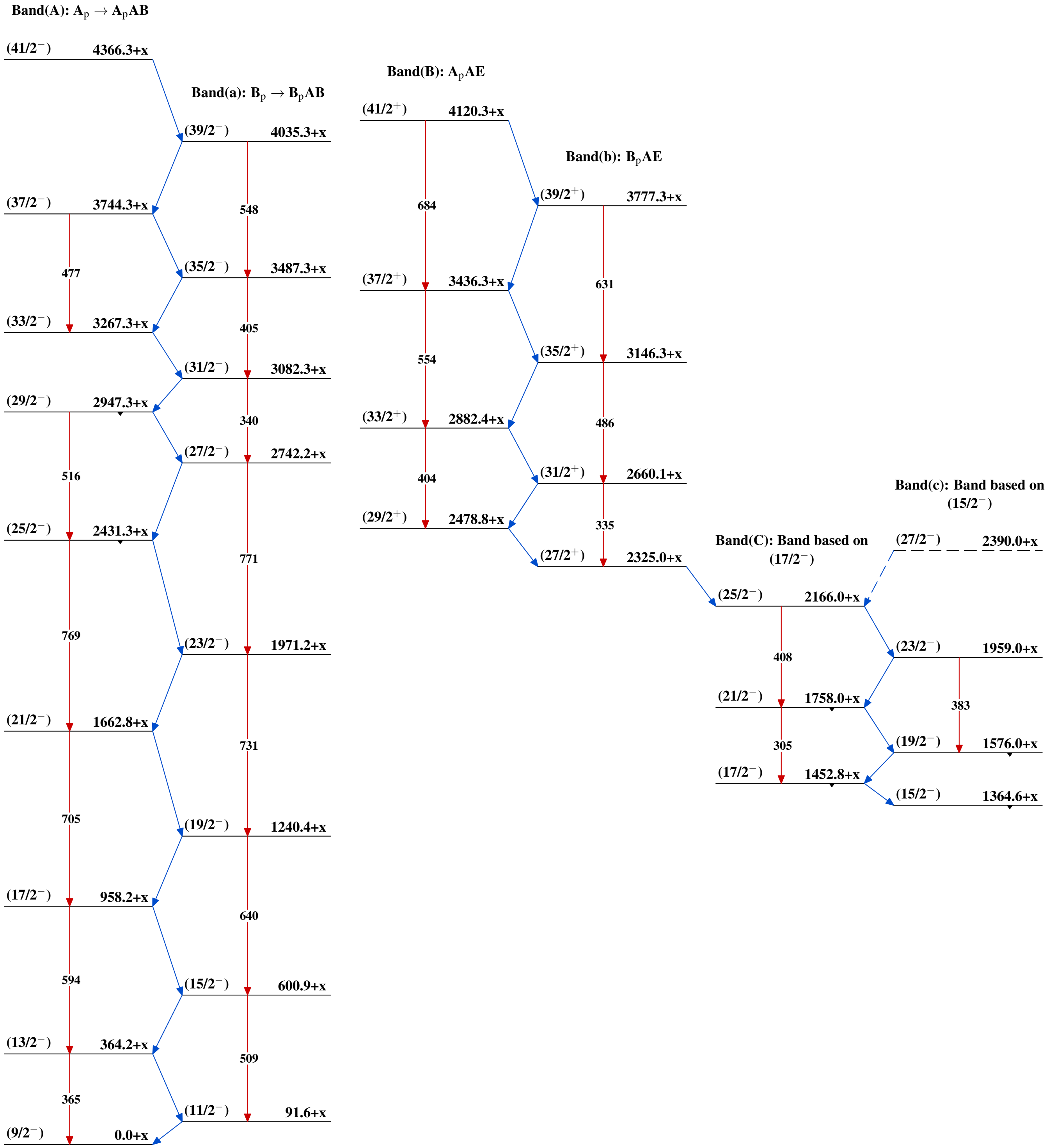

$^{167}_{75}Re_{92}$

$^{112}Sn(^{58}Ni,3p\gamma)$ 2003Jo06 (continued)